Spin Waves in the Ferromagnetic Ground State of the Kagome Staircase System $Co_3V_2O_8$

M. Ramazanoglu [1], C.P. Adams [1, 2], J.P. Clancy [1], A.J. Berlinsky [1, 3], Z. Yamani [4], R. Szymczak [5], H. Szymczak [5], J. Fink-Finowicki [5], and B.D. Gaulin [1, 3]

[1] Department of Physics and Astronomy, McMaster University, Hamilton, Ontario, Canada L8S 4M1
[2] Department of Physics, St. Francis Xavier University, Antigonish, Nova Scotia, Canada B2G 2W5
[3] Canadian Institute for Advanced Research, Toronto, Ontario, Canada M5G 1Z8
[4] Canadian Neutron Beam Centre, National Research Council, Chalk River Laboratories, Chalk River, ON, Canada K0J 1J0
[5] Institute of Physics, Polish Academy of Sciences, Warsaw, Poland 02-668

Magnetic materials in which the constituent magnetic moments reside on networks of triangles and tetrahedra have been of great interest due to their propensity for exotic ground states, a consequence of geometrical frustration [1]. While ferromagnetically-coupled moments on such lattices generally do not result in such ground states, ferromagnets, and materials that display both ferromagnetic (FM) and antiferromagnetic (AFM) interactions on such lattices remain of great interest, in part due to the relative scarcity of well-studied examples, and in part due to intriguing spin ice [2] and multiferroic phenomena [3] which characterize some of these ground states.

The kagome lattice is comprised of a two-dimensional network of corner-sharing triangles. Several realizations of magnetic moments on stacked kagome lattices with varying degrees of crystalline order have been extensively studied. The stacked kagome staircase materials $M_3V_2O_8$ (M = Ni, Co) display orthorhombic crystal structures with space group *Cmce* [4]. Their kagome layers are buckled and composed of edge-sharing $M^{2+}O_6$ octahedra. These layers are separated by non-magnetic $V^{5+}O_4$ tetrahedra. The buckled kagome layers are perpendicular to the orthorhombic *b*-axis and form what is known as a stacked kagome staircase structure. Figure 1 shows the projection of the kagome staircase onto the *a-c* plane. The two inequivalent M sites are known as spines (M1) and cross-ties (M2). The superexchange interaction between spine and cross-tie sites and between two adjacent spine sites are denoted by J_{sc} and J_{ss}, respectively.

One member of this family, $Ni_3V_2O_8$ (NVO), undergoes a series of phase transitions on lowering temperature [5-9]. A very interesting characteristic of this compound is that it exhibits simultaneous ferroelectric and incommensurate AFM order, that is, multiferroic behaviour, in one of its ordered phases. In isostructural $Co_3V_2O_8$ (CVO), the $S = 1$ magnetic moments at the Ni^{2+} site are replaced with $S = 3/2$ Co^{2+} moments. CVO also displays a rich low temperature phase diagram, which has been studied using polarized and unpolarized neutron diffraction, dielectric measurements [10], magnetization [11, 12] and specific heat measurements [12]. There is a series of four AFM ordered phases below T_N = 11.3 K which can be characterized by incommensurate or commensurate ordering wavevectors (0, τ, 0). In contrast to NVO, the ultimate ground state in CVO is ferromagnetic and the Curie temperature is $T_C \sim 6$ K. Earlier powder neutron diffraction measurements [10] on CVO showed ordered magnetic moments of 2.73(2) and 1.54(6) μ_B on the spine and cross-tie sites, respectively, at 3.1 K. All moments are aligned along the *a*-axis direction. In this experiment, we performed inelastic neutron scattering measurements of the spin wave excitations within the kagome staircase plane in the ferromagnetic ground state of single crystal CVO. These measurements are compared with linear spin wave theory and show a surprising sublattice dependence to the exchange interactions.

A large (5 g) and high-quality single crystal of CVO was grown using an optical floating-zone image furnace [12]. Thermal INS measurements were performed using the C5 triple-axis spectrometer. A pyrolytic graphite (PG) vertically-focusing monochromator and flat analyzer were used. Measurements were performed with a fixed final neutron energy of E_f = 13.7 meV and a PG filter in the scattered beam. The collimation after the monochromator was 29'-34'-72' resulting in an energy resolution of 0.9 meV FWHM. The crystal was oriented with the (h0l) kagome staircase plane coincident with the scattering plane. Constant-Q energy scans were performed along the high symmetry (h00) and (00l) directions in this plane. A follow up measurement was conducted using N5 triple-axis spectrometer with similar conditions.

A series of constant-Q scans for (h00) and (00l) directions were collected at T = 3 K and are presented as a color contour map in Figures 2a,c. Dispersive features corresponding to two bands of spin waves are seen in both data sets. The top of the upper spin-wave band at $\Delta E \sim 5.7$ meV corresponds to excitations reported earlier using a time-of-flight technique [7]. These constant-Q scans were fit to resolution-convoluted damped harmonic oscillator (DHO) lineshapes, which gave intrinsic energy widths for the higher-energy spin-wave mode at all wavevectors ranging from Γ = 0.6 to 1.1 meV, while the lower-energy spin waves were resolution limited at all wavevectors. This indicates a finite lifetime for the higher-energy spin waves even at temperatures ~ $T_C/2$.

We have carried out a linear spin-wave theory analysis of the magnetic excitations observed in Figures 2 (a) and (c) to understand as much of the relevant microscopic spin Hamiltonian as possible. The full Hamiltonian is potentially complicated if account is taken of the two inequivalent magnetic sites and the 3D kagome staircase structure. We employed a 2D model in which the magnetic ions in a layer are projected onto the average plane of the layer (Figure 1) and only near-neighbor exchange and single-ion anisotropy are included. Details about this theoretical calculation can be found elsewhere [13]. Best agreement between the experimental data and the spin-wave theory calculation in Figure 2 was obtained for magnetic coupling predominantly between the spine and cross-tie Co ions with J_{sc} = 1.25±0.08 meV, while the spine-spine coupling J_{ss} vanishes. Figure 2 shows that the spin-wave theory gives a very good description of the dispersion of the two modes (dashed lines) and accounts for the observed trend of the spin waves to trade intensity as a function of *Q*. This description is not perfect, however. The calculated dispersion of the lower spin-wave band is low compared with experiment near (200) and (002) where the intensity is very weak. The calculation is not convolved with the instrumental resolution; instead the energy width is manually set in both high and low-energy bands to correspond to the measured width. The broad (in energy) neutron groups corresponding to the upper spin-wave bands are most evident near (200) and (002). The lower energy spin-wave band becomes much more intense near the zone centers of (400) and (004). Steep excitation branches near (400) and (004) with comparatively weak intensity (Figures 2a,c) are identified as longitudinal acoustic phonons, with a speed of sound of 1050±100 m/s, in both directions. Interestingly, the upper spin wave band appears to hybridize with, or otherwise damp the longitudinal phonons near (004) (see Fig. 2c). This evidence for strong spin-lattice coupling is consistent with reports of a strong dielectric anomaly at $T_C \sim 6$ K for $\mathbf{E}\|(00L)$ [10].

Our INS study of the spin-wave excitations in the ferromagnetic ground state of CVO within its kagome staircase plane reveals two separate spin-wave bands between 1.6 and 5.7 meV. The upper spin-wave band is damped with finite energy widths Γ in the range of 0.6 to 1.1 meV. These spin-wave excitations can be accurately described by a simple model Hamiltonian and linear spin-wave theory. The model gives a magnetic coupling that is predominantly between the spine and cross-tie sites of the kagome staircase.

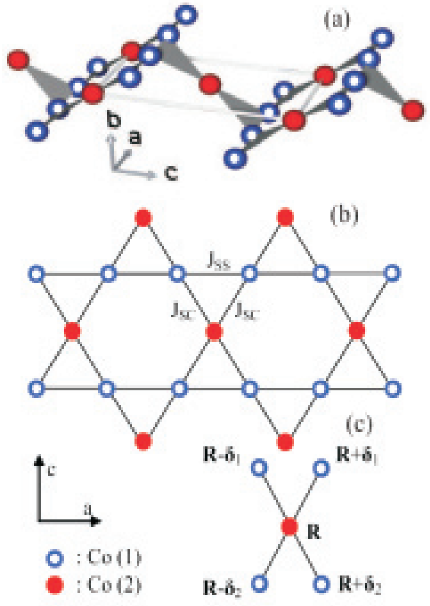

Fig. 1 Schematic diagrams of the kagome staircase structure in 3D (a) and as reduced to 2D (b) in the *a-c* plane. The cobalt ions are represented by open and solid circles for spine (*M1*) and cross-tie sites (*M2*), respectively. Chains of spine sites running parallel to the *a*-direction are alternatively above and below the plane. (c) The basis used in the linear spin-wave theory calculation.

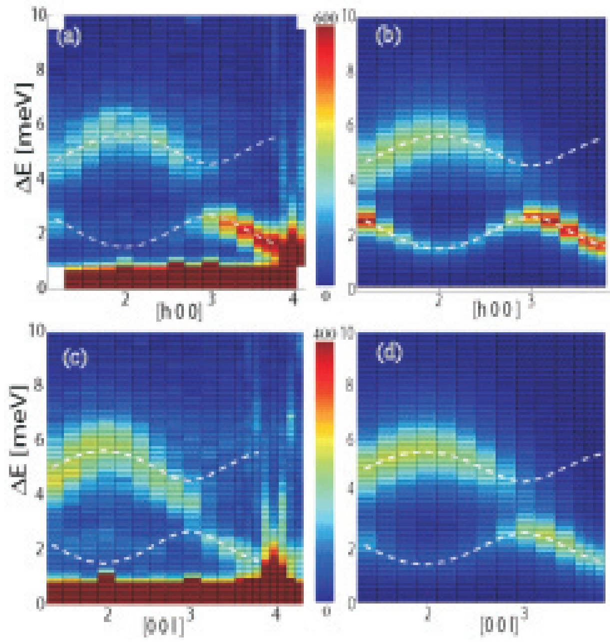

Fig. 2 Contour maps of INS at *T* = 3 K [(a) and (c)] and corresponding linear spin-wave theory [(b) and (d)] as described in the text. The broken lines show the dispersion relations resulting from this spin-wave theory analysis.

References

[1] Frustrated Spin Systems, Ed. H.T. Diep. World Scientific Publishing: Singapore, 2004.

[2] S.T. Bramwell and M.J.P. Gingras, Science 294, 1495 (2001).

[3] T. Kimura et al., Nature 426, 55 (2003); Nicola A. Hill, J. Phys. Chem. B 104, 6694 (2000).

[4] E.E. Sauerbrei *et al.*, Acta Cryst.B. 29, 2304 (1973).

[5] M. Kenzelmann *et al.*, Phys. Rev. B 74, 014429 (2006).

[6] G. Lawes *et al.*, Phys. Rev. Lett. 93, 247201, (2004).

[7] N.R. Wilson *et al.*, J. Magn. and Magn. Mat. 310, 1334 (2007).

[8] N. Rogado *et al.*, Solid State Comm. 124, 229 (2002).

[9] T. Lancaster *et al.*, Phys. Rev. B 75, 064427 (2007).

[10] Y. Chen *et al.*, Phys. Rev. B 74, 014430 (2006).

[11] G. Balakrishnan *et al.*, J. Phys.: Condens. Matter 16, L347 (2004).

[12] R. Szymczak *et al.*, Phys. Rev. B 73, 094425 (2006).

[13] arxiv.org. 0804.1929.